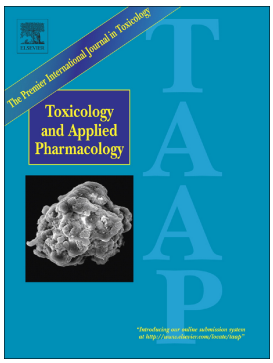

Erianin, a novel dibenzyl compound in Dendrobium extract, inhibits bladder cancer cell growth via the mitochondrial apoptosis and JNK pathways

Qiyu Zhu, Yuwen Sheng, Wenhua Li, Jing Wang, Yulin Ma, Baowen Du, Yaxiong Tang

PII: S0041-008X(19)30117-6
DOI: https://doi.org/10.1016/j.taap.2019.03.027
Reference: YTAAP 14555

To appear in: *Toxicology and Applied Pharmacology*

Received date: 14 November 2018
Revised date: 29 March 2019
Accepted date: 30 March 2019

Please cite this article as: Q. Zhu, Y. Sheng, W. Li, et al., Erianin, a novel dibenzyl compound in Dendrobium extract, inhibits bladder cancer cell growth via the mitochondrial apoptosis and JNK pathways, Toxicology and Applied Pharmacology, https://doi.org/10.1016/j.taap.2019.03.027

Erianin, a novel dibenzyl compound in *Dendrobium* extract, inhibits bladder cancer cell growth via the mitochondrial apoptosis and JNK pathways

Qiyu Zhu[a,1], Yuwen Sheng[a,1,*] shengyuwen0326@163.com, Wenhua Li[a], Jing Wang[a], Yulin Ma[a], Baowen Du[a], Yaxiong Tang[a,*] tangyx@cib.ac.cn

[a]Chengdu Institute of Biology, Chinese Academy of Sciences, Chengdu 610041, China

[b]University of Chinese Academy of Sciences, Beijing 100000, China

[*]Corresponding authors.

Abstract

Erianin, a component extracted from the traditional Chinese herbal medicine *Dendrobium*, has shown significant anti-tumour activity in various cancers but not in bladder cancer. In this study, we assessed the effects of Erianin on bladder cancer growth and elucidated the related mechanisms. First, Erianin was synthesized with

[1] These authors contributed equally to this work.

high yields, and markedly suppressed EJ and T24 cell proliferation. It induced G2/M-phase arrest *in vitro*. Furthermore, Erianin triggered apoptosis via caspase cascades activation and the mitochondrial-mediated apoptotic pathway. Bim up-regulation and Bcl-2 down-regulation as the symbol of apoptosis which were found to play the dominant role in the effects of Erianin. We further showed that JNK pathway activation is necessary for the Erianin-mediated anti-proliferation and apoptotic response. Finally, Erianin exhibited anti-tumour activity and induced apoptosis in tumour tissue *in vivo*. Collectively, these results suggest that Erianin induced cell cycle G2/M-phase arrest and apoptosis via the JNK signalling pathway in bladder cancer, indicating the potential usefulness of Erianin for the therapy of bladder cancer.

Keywords: Erianin, Bladder cancer, Apoptosis, JNK pathway, *In vivo*.

1. Introduction

Bladder cancer is the most common and uncontrollable heterogeneous tumour worldwide (Jin et al., 2015). According to American cancer statistics, an estimated 79,030 new cases and 16,870 deaths in the United States in 2017 will be due to bladder cancer (Siegel et al., 2017). At present, surgical resection and chemotherapy

are the most common bladder cancer treatments and are widely used throughout the world (Marta et al., 2012). However, due to poor diagnosis, these treatments have little effect on 70% of bladder cancer patients presenting with superficial tumours (Zhang et al., 2016). The five-year recurrence rate for bladder cancer patients remains at 50~70% (Jones et al., 2000). Targeted therapy, which is known to exhibit low toxicity and high efficiency, has become an area of great interest for cancer treatment. Some targeted drugs, such as Atezolizumab and Avelumab (Krishnamurthy et al., 2017; Vandeveer et al., 2016), have shown promising results in bladder cancer treatment. However, targeted therapy is limited in bladder cancer by unclear targets. Therefore, more chemopreventive and chemotherapy drug candidates are urgently needed for controlling bladder cancer progression.

Apoptosis is an evolutionary process that occurs after physiological and pathological stimulation and induces programmed cell death (Elmore, 2007). This process involves morphological and biochemical changes, such as membrane blebbing, DNA fragmentation, chromatin condensation, protein cleavage, et al (Kalimuthu and Se-Kwon, 2013). Furthermore, apoptosis is accompanied by the activation of the extrinsic and intrinsic apoptosis pathways and other pathways. The extrinsic pathway, also called the death receptor pathway, is initiated when the death receptor Fas is activated and initiated caspase cascades (Kantari and Walczak, 2011). The intrinsic pathway, which is also known as the mitochondria-dependent pathway, is primarily regulated by the Bcl-2 protein family and mediated apotosis by a release of mitochondrial cytochrome *c* (Sawada et al., 2000). In addition, the JNK pathway is

the crucial role in cell survival and apoptosis (Son et al., 2011). In response to an apoptosis signal, JNK rapidly moves to the mitochondrial membrane and induces cytochrome *c* release (Tobiume et al., 2001). In addition, JNK can activate Bim and then activate Bax or Bak, thus inducing apoptosis (Marani et al., 2002). Many previous reports have shown that cell survival inhibition and apoptosis induction by therapeutic agents might be correlated with the tumour response, and some drugs have shown significant inhibition of bladder cancer by inducing apoptosis (e.g., Artesunate and Naproxen) (Zuo et al., 2014; Kim et al., 2014). Thus, using agents to promote cell apoptosis is a promising strategy for bladder cancer treatment.

The medicinal value of plants has been recognized by many cultures and most human societies for millennia. The chemical diversity in the natural world are unsurpassed by synthetic compounds (Davison EK and Brimble MA, 2019). Many phytochemicals have been used for cancer treatment in human clinical trials and have shown promising anti-cancer effects due to their low toxicity, safety, and general availability (Gupta et al., 2001). Modern pharmacological studies have found that *Dendrobium* contains various chemical components with extensive pharmacological effects (Huang et al., 2016; Li et al., 2018; Yuan et al., 2019). Erianin is a low-molecular-weight natural product extracted from *Dendrobium chrysotoxum* (Ma et al., 1994) and belongs to the stilbene dihydrostilbene derivative family named combretastatins, which consistently exert anti-proliferative effects on carcinoma cell lines (Ma et al., 1994). Similarly, Erianin has been reported to exert an obvious inhibitory effect on cell proliferation and a promotive effect on apoptosis in liver

cancer, colon cancer, gastric carcinoma and leukaemia HL-60 cells (Li et al., 2001). However, to the best of our knowledge, neither the mechanism nor the effect of Erianin on bladder cancer have been reported. Hence, in this study, we assessed the anti-tumour potential and molecular mechanisms of Erianin in human bladder cancer EJ and T24 cells and explored the potential value of Erianin application for chemoprevention and bladder cancer therapy.

2. Materials and methods

2.1 Compounds

Erianin was synthesized from 3,4,5-trimethylbenzaldehyde. The intermediate product bromotriphenyl(3,4,5-trimethoxybenzyl)-phosphane was obtained through

borohydride reduction and the Michaelis-Arbuzov reaction and was then was reacted with the hydroxyl groups of isovanillin through Wittig, borohydride reduction and dehydroxylation reactions, yielding a white powder that was identified as Erianin (1.49 g, 95%, purity 98.5%). ^{1}H NMR (400 MHz, $CDCl_3$) δ 6.81 (d, J = 1.9 Hz, 1H), 6.77 (d, J = 8.2 Hz, 1H), 6.64 (dd, J = 8.2, 1.9 Hz, 1H), 6.38 (s, 2H), 5.59 (s, 1H), 3.87 (s, 3H), 3.83 (d, J = 1.2 Hz, 9H), 2.82 (s, 4H).

Pure Erianin was dissolved in dimethyl sulfoxide (DMSO) and stored at -80°C.

2.2 Reagents

3-(4,5-dimethylthiazol-2-yl)-2,5-diphenyltetrazolium bromide (MTT) were obtained from Sigma-Aldrich (St. Louis, MO, USA). 4,6-diamino-2-phenyl indole (DAPI), the JNK inhibitor SP600125, the caspase inhibitor Z-VAD-FMK, Annexin V-FITC detection kit, a One-Step TUNEL Apoptosis Detection Kit were purchased from Beyotime (Shanghai, China). The cell cycle assay kit, the mitochondrial membrane potential kit (JC-1), the cytochrome *c*-releasing apoptosis assay kit were purchased from KeyGEN BioTECH (Nanjing, China). Primary antibodies against β-actin, p-Chk2, p-cdc2, p-H2A.X, p-cdc25C, PARP, caspase-9, caspase-7, caspase-3, cytochrome *c*, COX IV, Bim, Bik, Bax, Bad, BID, Bcl-2, Mcl-1, p-JNK1/2, p-c-Jun and p-Bcl-2 were purchased from Cell Signalling Technology (Beverly, MA, USA). Chemiluminescence detection reagents were obtained from Millipore (Plano, TX, USA). Lipofectamine 2000 were purchased from Invitrogen (Carlsbad, CA, USA).

2.3 Cell culture

The human bladder cancer cell lines EJ and T24 were obtained from State Key Laboratory of West China Hospital Cancer Center, Sichuan University, China. EJ and T24 cells were cultured in RPMI-1640 medium containing 1% penicillin-streptomycin and 10% (v/v) FBS in moist air with 5% CO_2 at 37°C.

2.4 Cell proliferation assay

Cell proliferation was examined through MTT assays. Briefly, EJ and T24 cells were seeded into 24-well plates at 2×10^4 cells per well and incubated for 24 h. After treatment, the cells were incubated for 48 h, then 0.5 mL of MTT solution (final concentration of 1 mg/mL) was added to each well and incubated for 4 h. The MTT solution was then removed, and 0.5 mL of acidified isopropanol (with 0.4% HCl) was added to solubilize the formazan crystals. Three replicates were performed, and the OD_{570} was analysed using a microplate reader (BD Biosciences, Mountain View, CA, USA). The ratio of viability (%) was calculated as $OD_{sample}/OD_{control} \times 100\%$.

2.5 Cell cycle synchronization analysis

The cell cycle synchronization of EJ and T24 cells was achieved by serum starvation. The cells were treated with serum-free medium for 24 h, pretreated with Z-VAD-FMK (20 μM) and SP600125 (10 μM) for 2 h, and then treated with Erianin for 24 h. The cells were harvested, fixed with 70% (v/v) ethanol overnight at -20°C and washed with PBS and then labelled with propidium iodide (50 μg/mL) and incubated at RT in the dark for 30 min. Approximately 10000 cells in each sample were analysed with a FACScan flow cytometer (BD Biosciences, Mountain View, CA,

USA), and the percentages of cells in the G1, S, and G2/M cell cycle phases were investigated using ModFIT software as described previously (Tang et al., 2008).

2.6 Cell morphology observation and DAPI staining

EJ and T24 cells in the logarithmic phase were plated in six-well culture plates. after the cells adhered to the plate, After Erianin treatments for 24 h, the medium was removed, and the cells were washed three times with PBS. The cells were then observed and photographed using an inverted microscope (Olympus, Tokyo, Japan). The cells were inoculated on a cover slip treated with Erianin. After the treatments, the cells were fixed with 4% paraformaldehyde for 30 min and stained with 1 μg/mL DAPI for 5 min. Finally, the cells were observed with a fluorescence microscope (Olympus, Tokyo, Japan) using emission and excitation wavelengths of 460 nm and 350 nm, respectively.

2.7 Annexin V/PI analysis

To quantify the cell death modality, EJ and T24 cells were stained using an Annexin V-FITC detection kit. Cells in the exponential growth phase were seeded in 60-mm^2 dishes, incubated at 37 ℃ for 24 h, pretreated with Z-VAD-FMK (20 μM) and SP600125 (10 μM) for 2 h, and then treated with Erianin for 24 h. The cells were then collected, washed twice with PBS, resuspended in 400 μL of Annexin binding buffer, stained with 5 μL of Annexin V-FITC and 10 μL of PI, and incubated for 15 min at RT in the dark. The stained cells were analysed with a FACScan flow cytometer (BD Biosciences, Mountain View, CA, USA), and the percentages of

apoptotic cells were investigated using FlowJo software.

2.8 Analysis of mitochondrial membrane potential

To investigate the mitochondrial membrane potential, a mitochondrial membrane potential kit (JC-1) was used. EJ cells were seeded into six-well culture plates, incubated overnight and treated with various concentrations Erianin for 24 h. The medium was then removed, 1 mL of JC-1 dye working solution was added (according to the manufacturer's recommended protocol), and the cells were incubated for 20 min at 37°C. After incubation, the cells were washed twice with JC-1 dyeing buffer, and then, 2 mL of cell culture medium was added. Cell staining was observed with a fluorescence microscope or analysed with a flow cytometer.

2.9 Measurement of cytochrome c release from mitochondria

Cells were treated with Erianin for 24 h. The cytosol and mitochondria were separated using a cytochrome *c*-releasing apoptosis assay kit. The cells were suspended in cytosol extraction buffer, mixed in a Dounce homogenizer, and centrifuged (700 × g) for 10 min at 4°C. The supernatant was collected and recentrifuged (10,000 × g, 30 min) at 4°C. The pellet (mitochondrial fraction) and supernatant (cytosolic fraction) were used for western blot analysis.

2.10 Western blot analysis

EJ and T24 cells were lysed in ice-cold radioimmunoprecipitation (RIPA) buffer (50 mmol/L Tris, pH 7.4, 150 mmol/L NaCl, 1% NP-40, 0.5% sodium deoxycholate, 0.1% sodium dodecyl sulphate (SDS), 1 mmol/L ethylenediaminetetraacetic acid

(EDTA), and 1% protease inhibitor cocktail (v/v)). Total protein (40–80 μg) was separated by SDS–PAGE and then transferred to nitrocellulose membranes. The membranes were blocked with 5% non-fat milk for 1 h, labelled with primary antibodies overnight at 4°C, subjected to four 10-min washed with PBS with Tween (PBST), and incubated with horseradish peroxidase-conjugated secondary antibody for 1–2 h at RT. According to the manufacturer's recommended protocol, the target proteins were then detected via enhanced chemiluminescence.

2.11 Plasmid transfection

The pcDNA3.1, pcDNA3.1-Bcl-2-V5-tag and pCMV-TAM67 plasmids were generous gifts from Dr. Xiaolin Zi (University of California Irvine, Orange, CA, USA). EJ and T24 cells were plated in 24-well plates and transiently transfected with pcDNA3.1, pcDNA3.1-Bcl-2-V5-tag or pCMV-TAM67 using Lipofectamine 2000, and 48 h after transfection, the cells were treated with Erianin 48 h after transfection.

2.12 RNA interference

The Bim-targeting sequences were designed using the RNAi Designer programme, and the RNAi cassettes were cloned into a PENTR™/U6 Entry vector and subsequently transferred into a pBLOCK-iT™3-DEST vector using Clonase™ to catalyse a recombination reaction (Invitrogen, Carlsbad, CA, USA). The following Bim-targeting sequence was selected for further studies: 5'-GGAGACGAGTTTAACGCTTAC-3'. Prior to the experiment, 4×10^4 EJ and T24 cells were seeded in each well of a 24-well plate. When the cells reached

approximately 60% confluence, they were transfected with shRNA using Lipofectamine 2000.

2.13 In vivo tumour model

NCR-nu/nu (nude) mice were purchased from Taconic, and the animal experiments were approved by the Committee of Animal Ethics of Chengdu Institute of Biology, Chinese Academy of Sciences, China (#CIBCAE20160814), and were performed in strict accordance with the Guide for the Care and Use of Laboratory Animals of the Ministry of Health, China. At the end of the animal experiment, the animals were sacrificed via cervical vertebral dislocation to reduce the pain of the animals. Erianin was dissolved in 10% grain alcohol in 0.9% saline and administered via gavage to the mice. Then, 2×10^6 EJ cells per 100 μL of PBS were injected s.c. into the right flank of the nude mice. The tumours grew to approximately 120 mm^3 after seven days, and the mice bearing EJ tumours were randomly divided into the control and treatment groups, with 10 mice in each group, and dosed daily with vehicle or 50 mg/kg Erianin. Because no in vivo data regarding s.c. Erianin administration are mentioned in the literature (only i.p. injections are described) (Wang et al., 2016; Yu et al., 2016), the Erianin dose (50 mg/kg) used in this study was based on the pharmacologically effective and non-toxic doses of other compounds determined in our laboratory. The water consumption, diet and body weight were recorded thrice weekly. Once xenografts started growing, the tumour size was measured every three days, and the volume was calculated using the formula $0.5236\ L_1\ (L_2)^2$, where L_1 is the long axis and L_2 is the short axis of the tumour. At the

end of the experiment, the tumours were removed, weighed, and stored at −80°C.

2.14 TUNEL assay

For detection of the apoptotic induction effect, we used a One-Step TUNEL Apoptosis Detection Kit according to the manufacturer's recommended protocol. Briefly, the samples were fixed with 4% formaldehyde solution for 40 min, washed twice in PBS treated with 0.1% Triton X-100 in PBS and incubated on ice for 2 min. The reaction mix was prepared according to the manufacturer's recommended protocol. After two washes in PBS, staining was performed at 37°C for 60 min away from light, and the resulting staining was observed with a fluorescence microscope (Olympus, Tokyo, Japan).

2.15 H&E staining

At the end of the study, tumour tissues were harvested from each mouse and fixed in 10% phosphate-buffered formalin for 24 h. The formalin-fixed tissues were paraffin-embedded, sectioned, and stained with H&E. The sections were evaluated for the degree of tumour cell apoptosis, and the apoptotic cells were counted under a microscope.

3. Results

3.1 Erianin inhibited human bladder cancer cell proliferation but had minimal effects on normal cells

Erianin is a natural compound primarily extracted from the precious traditional Chinese herb *Dendrobium*; however, considering the low extract yield, Erianin was synthesized in this study from 3,4,5-trimethylbenzaldehyde using a series of reactions, including hydroboration, Michaelis-Arbuzov, and Witting reactions (Fig. 1A) (Cushman M, et al., 1991) with an excellent yield (95%). The structure of Erianin was confirmed by nuclear magnetic resonance spectroscopy, and the final product was of analytical grade (Supporting Information Figs. A and B in S1 File).

To investigate the inhibitory effects and cytotoxicity of Erianin in bladder cancer cells, EJ and T24 cells were treated with various Erianin concentrations for 48 h and then subjected to MTT assays. As shown in Fig. 1B, Erianin inhibited EJ and T24 cell growth in a dose-dependent manner. The IC_{50} values of Erianin in the EJ and T24 cell lines were estimated to equal 65.04 nM and 45.9 nM. However, Erianin had a minimal effect on normal liver cell growth. The selective killing effect of Erianin on bladder cancer cells over normal cells suggest its potential value for bladder cancer treatment.

3.2 Erianin induced G2/M arrest in EJ and T24 cells

To explore whether the proliferation inhibition effect of Erianin was induced through disruption of cell cycle progression, a flow cytometry analysis was performed to examine the cell cycle distribution. The results indicated that the relative percentage of cells in the G2/M phase increased from 3.00% in the control population of EJ cells to 55.0% in the population of EJ cells treated with different Erianin

concentrations (40, 80, or 160 nM) ($P < 0.05$) and from 8.29% in the control population of T24 cells to 51.9% in the population of T24 cells treated with various Erianin concentrations (25, 50, 100 nM) (Fig. 2A-2B), and these increases were accompanied by decreases in the numbers of cells in the G0/G1 phases. However, Erianin couldn't induce the cell cycle arrest in the normal liver LO2. Furthermore, a western blotting analysis was performed to examine the protein profile of cell cycle markers and DNA damage response proteins. The results showed that phospho-Chk2, phospho-cdc2 and phospho-H2A.X expression was up-regulated and the level of phospho-Cdc25c was down-regulated (Fig. 2C), but Erianin not induced the expression change of phospho-Chk2, phospho-cdc2, phospho-H2A.X and phospho-Cdc25c in LO2 cells, indicating that Erianin induced G2/M cell cycle arrest by modulating cell cycle-related protein expression in EJ and T24 cells but not in the normal liver LO2 cells. In addition, we used the different dose range for EJ cells and T24 cells because of the different IC_{50} values of Erianin in both cells.

3.3 Erianin inhibited EJ and T24 cell proliferation by inducing apoptosis

Apoptosis is a crucial event in tumour cell fate decisions. To explore whether the proliferation inhibition effect of Erianin was related to apoptosis induction, DAPI staining was performed to investigate morphological changes in bladder cancer cells treated with Erianin. The Erianin-treated cells exhibited a typical apoptotic morphology, including cell shrinkage, nuclear changes, and chromatin fragmentation, whereas these characteristics were not observed in control cells (Fig. 3A) and LO2 cells(Fig. S4). To further verify a causal relationship between cell growth inhibition

and apoptosis, the effects of Erianin on apoptosis and cell death in bladder cancer cells were examined by Annexin V-FITC/PI staining followed by flow cytometric analysis. Erianin treatment significantly increased the number of apoptotic cells compared with the control treatment (Fig. 3B). Furthermore, treatment of the cells with the combination of Erianin and Z-VAD-FMK (20 μM) conspicuously decreased the number of apoptotic cells and the reversed induced G2/M cell cycle arrest (Fig. 3C). Nevertheless, Erianin treatment not increased the number of apoptotic cells compared with the control treatment(Fig. S6) in LO2. The activation of caspase cascades plays an executive role in the apoptosis process. As shown in Fig. 3D, Erianin induced activation of caspase-9/7/3 cleavage, thus inducing caspase cascades and eventually leading to PARP cleavage in both EJ and T24 cells, but Erianin couldn't induce PARP cleavage in LO2 cells(Fig.S6). Furthermore, the caspase inhibitor Z-VAD-FMK (20 μM; the Z-VAD-FMK dose response curve in EJ and T24 cells is shown in Supporting Information Fig. 2A in S1 File) was used to intervene with Erianin-induced apoptosis in bladder cancer cells. Consistently, the treatment of bladder cancer cells with the combination of Erianin and Z-VAD-FMK significantly decreased the number of cells (Fig. 3E). Hence, the proliferation inhibition effect of Erianin is primarily associated with apoptosis induction through activation of caspase cascades.

3.4 Erianin induced cytochrome c release and related changes in the mitochondrial membrane potential in bladder cancer cells

Apoptosis can be induced by the extrinsic pathway, which is associated with

death receptor stimulation on the cell surface, or by the intrinsic pathway, which is characterized by mitochondrial dysfunction. To explore whether apoptosis induced by Erianin was related to the intrinsic pathway characterized by mitochondrial involvement, the effect of Erianin on mitochondrial membrane potential was determined using the mitochondrial probe JC-1. A fluorescence microscopy analysis indicated that Erianin markedly enhanced green fluorescence compared with that observed in the control group, whereas a flow cytometry analysis showed that 55% of EJ cells presented an altered membrane potential compared with the control cells after treatment with 160 nM Erianin (Fig. 4A-4B).

Furthermore, considering the crucial role of cytochrome *c* release in the mitochondrial-related intrinsic pathway, cytochrome *c* expression in the mitochondria and cytoplasm was examined by western blotting. The results showed that in both EJ and T24 cells, Erianin treatment induced cytochrome *c* release from the mitochondria into the cytosol (Fig. 4C), indicating that the mitochondrial-mediated apoptotic pathway was activated.

3.5 Erianin activated the mitochondrial-mediated apoptotic pathway by regulating the protein expression of Bcl-2 family members

Bcl-2 family members are important in the apoptosis process and include anti-apoptotic and pro-apoptotic proteins, and regulation of the delicate balance among these members determines cell fate. The expression of the pro-apoptotic proteins Bik, Bax, Bim, BID and Bad and the anti-apoptotic proteins Mcl-1 and Bcl-2

in EJ, T24 and LO2 cells treated with 0.1% DMSO or Erianin was investigated by western blotting. The results indicated that Erianin up-regulated Bim, Bik, BID and Bad and clearly down-regulated Bcl-2 and Mcl-1 but had no effect on Bax in EJ cells. In T24 cells, Erianin up-regulated Bim and Bad and down-regulated Bcl-2 (Fig. 5A). However, the expression of pro-apoptotic proteins Bik, Bax, Bim, BID and Bad and the anti-apoptotic proteins Mcl-1 and Bcl-2 were unchanged in LO2 compared with control. Taken together, these results indicate that Erianin activated the mitochondria-mediated apoptotic pathway by regulating the balance between pro-apoptotic and anti-apoptotic protein expression.

In addition, given that Bim up-regulation and Bcl-2 down-regulation were confirmed in both EJ cells and T24 cells, we further examined their roles in the growth inhibitory effect of Erianin. EJ and T24 cells were subjected to the knockdown of Bim via short hairpin RNAs and the overexpression of Bcl-2 followed by Erianin treatment (40 nM, 80 nM, or 160 nM (EJ cells) and 25 nM, 50 nM, or 100 nM (T24 cells)) for 48 h, and cell proliferation was then measured through MTT assays. Consistent with the above-described results, the suppression of Bim expression and the overexpression of Bcl-2 attenuated the growth inhibition effect of Erianin on bladder cancer cells (Fig. 5B-5C). These results suggest that Bim and Bcl-2 are, at least in part, required for the cell growth inhibition effect of Erianin.

3.6 Erianin induced apoptosis via JNK pathway activation

The JNK family plays a core role in the signalling pathways associated with cell

differentiation, proliferation and apoptosis. Therefore, to examine whether Erianin induced apoptosis through the JNK pathway, the cells were treated with Erianin only or pretreated with the JNK inhibitor SP600125 (10 μM; the SP600125 dose response curve for EJ and T24 cells is shown in Supporting Information Fig. B in S2 File) and then treated with Erianin. Western blotting results showed that treatment with Erianin activated JNK signalling through phospho-JNK, phospho-c-Jun and phospho-Bcl-2 (Ser70) up-regulation. However, the JNK inhibitor SP600125 potently inhibited the JNK pathway activation induced by Erianin (Fig. 6A) in EJ cells. Next, to verify the effect of JNK pathway activation on Erianin-induced growth inhibition, the cells were first pretreated with SP600125 and then treated with Erianin for an additional 24 h. As shown in Fig. 6B, pretreatment with SP600125 clearly attenuated the inhibition of proliferation induced by Erianin. Furthermore, the transient transfection of EJ cells with plasmid encoding dominant negative c-Jun (pCMV-TAM67) to inhibit c-Jun activation, the growth inhibition induced by Erianin was also attenuated (Fig. 6C). A flow cytometric analysis also indicated that SP600125 attenuated the Erianin-induced G2/M arrest (Fig. 6D), and Annexin V-FITC/PI staining showed that SP600125 reduced the apoptotic effect of Erianin (Fig. 6E). Taken together, these results confirmed that Erianin-induced activation of the JNK pathway plays a crucial role in the induction of both cell proliferation and apoptosis in EJ and T24 cells.

3.7 Erianin inhibited tumour growth in vivo

To further examine the anti-proliferation effects of Erianin in vivo, a xenograft mouse model was constructed through the subcutaneous transplantation of EJ cells.

After two weeks, the mice were orally administered 50 mg/kg Erianin daily for 24 days. The growth rate of EJ cell-derived tumours treated with Erianin significantly decreased compared with that of the control group ($P < 0.05$) (Fig. 7A). The wet tumour weights were measured, and the mean results for the control and Erianin-treated groups were 1479 ± 26 and 516 ± 2.3 mg, respectively. Erianin treatment reduced tumour growth by approximately 65% (Fig. 7B). Simultaneously, to examine the potential apoptosis-inducing effect of Erianin in tumour tissues, a TUNEL staining analysis was performed, and the results demonstrated a notable increase in DNA breakage in the Erianin-treated tumour tissues in comparison with the control group (Fig. 7C). Haematoxylin and eosin (H&E) staining of tumour tissues obtained at the end of the study showed that the untreated tumour cells and their nuclei exhibited an uneven staining intensity, and the morphology and eosin staining of the cytoplasm of the untreated tumour cells was lighter than that of Erianin-treated tumour cells; in addition, tissue from Erianin-treated mice exhibited intense eosinophilic staining, which indicated massive apoptosis of tumour cells (Fig. 7D). These data suggest that Erianin exhibited potent anti-tumour activity by inducing apoptosis in vivo.

4. Discussion

Natural medicinal plants are important sources for the research and development

of novel drugs due to the diversity of their biological sources and chemical structures. *Dendrobium* is commonly known as one of the largest and most important (medicinally and ornamentally) herbs in the Orchidaceae family (Teixeira et al., 2014), which includes various species that are extensively used as Chinese medicinal materials, such as *D. aphyllum, D. candidum, D. chrysanthum,* and *D. densiflorum* (Li et al., 2011; Ng et al., 2012). *Dendrobium* species have been reported to exert various bioactivities, including antioxidant, immunomodulatory, neuroprotective, anti-inflammatory, and strong anti-tumour activities, in hepatic carcinoma, lymphoma, and lung cancer (Gong et al.,2004; Prasad and Koch, 2014; Charoenrungruang et al., 2014). Erianin is the most abundant active component extracted from *Dendrobium* and shows significant anti-tumour activity in some human cancers, such as human osteosarcoma cells (Wang et al., 2016), but its effect on bladder cancer has not been previously examined. The cytotoxicity observed in this study indicated that Erianin clearly inhibited EJ and T24 cell proliferation but exhibited little cytotoxicity toward normal liver LO2 cells in vitro. In addition, Erianin inhibited in vivo tumour growth without obvious toxicity. Furthermore, our results showed that Erianin caused G2/M cell arrest and DNA damage, because of phospho-H2A.X in the sign of DNA damage. Cells instantaneously block cell cycle progression, to allow time for repair when DNA damage(Shaltiel IA, et al., 2015). Erianin could up-regulated the expression of phospho-Chk2, phospho-cdc2, phospho-H2A.X and down-regulated the expression of phospho-Cdc25c at 160 nM, indicating Erianin induced the G2/M arrest by DNA damage and induced apoptosis through the mitochondria-related intrinsic pathway and

that the JNK signalling pathway played a critical role. Thus, Erianin might have potential value for bladder cancer treatment due to its low toxicity and high apoptosis induction efficiency.

Cell death is commonly induced by apoptosis, necrosis or autophagy, but among these, apoptosis plays more important role in deciding cell fate, particularly in cancer cells. Apoptosis leads to substantial changes in cell morphology, such as membrane blebbing and cell shrinkage, and to DNA fragmentation, chromatin condensation and the formation of apoptotic bodies (Li et al., 2007). These changes were induced in the cells through activation of the caspase signalling pathway. Caspase family proteins are the critical executors of the apoptosis pathway. All caspases are initially present in inactivate zymogen form, and when cells receive apoptosis signals, the mitochondrial membrane potential decreases, cytochrome *c* is released from the mitochondria, and apoptotic bodies are formed. The apoptotic bodies activate the initiator caspase-9, which acts on the downstream target effector caspase-7/3 (Shi, 2002; Ohtsuka et al., 2003). Activated caspase-9/7/3 induces PARP cleavage, which is a hallmark of apoptosis and important in many cellular processes, such as DNA repair, cell death, chromatin function and genomic stability. PARP cleavage occurred via caspase-9/7/3 activation in Erianin-treated EJ and T24 cells. In addition to the caspase family, another protein family is known to be very important in the apoptotic process: Bcl-2 family proteins (Wang et al., 2007). The Bcl-2 family proteins include apoptosis-promoting proteins (e.g., Bim, BID, Bad, Bax, and Bik) and anti-apoptotic proteins (e.g., Bcl-2 and Mcl-1). Among these members, Bim has been demonstrated

to be essential and can indirectly induce Bax and Bak oligomerization on mitochondria, and polymeric Bax forms holes in liposomes through which cytochrome *c* is released into the cytoplasm to induce apoptosis. In this study, Erianin induced Bim up-regulation, and the silencing of Bim expression significantly rescued the proliferation inhibition effect of Erianin on EJ and T24 cells. Therefore, we speculate that Bim might be an important element for the growth inhibition and apoptosis induction effects of Erianin.

SAPK/JNK is a member of the MAPK family and is activated by multifarious environmental stressors, growth factors, inflammatory cytokines, and G protein-coupled receptors. Overwhelming evidence suggests that JNK plays an important role in cell proliferation, differentiation, apoptosis and other cell regulation processes. Activation of the JNK signalling pathway by phosphorylated JNK/c-Jun can promote mitochondrial cytochrome *c* release and induce mitochondrial-mediated apoptosis (Lai et al., 2011). In addition, activated JNK is transferred to the nucleus and trans-activates c-Jun, thereby up-regulating apoptotic precursor genes and inducing apoptosis (Chen, 2012). Previous studies have shown that Bim is a significant convergence point in apoptotic signalling regulated by AKT and ERK. The experimental results showed that erianin increased the p-JNK levels and induced c-Jun and Bcl-2 phosphorylation. Thus, the JNK pathway is involved in the Erianin-mediated apoptotic response in bladder cancer.

Compared with traditional chemotherapy and radiation therapy, targeted tumour therapy has the benefits of high specificity and low toxicity. However, few targeted

anti-cancer drugs have been developed. Drug discovery typically takes one of two approaches: phenotypic screening or a target-based approach. Phenotypic screening involves small molecule libraries that are filtered against live cells with a phenotypic output. However, this method has challenges, such as poor cell uptake or cell removal of the compound and non-specific cytotoxicity effects. The target-based approach has many advantages, including known compound patterns of action and the ability to design compounds through a guiding structure. Therefore, molecular target screening has become the main early drug discovery method. Natural products, as the basis of drug development, have been widely applied in clarifying cellular mechanisms and drug development. In our study, we demonstrated that Erianin exerts significant inhibitory effects on bladder cancer cells and low toxicity toward normal liver cells, which hints at the huge potential of Erianin and its targets for drug development. Therefore, the identification of Erianin targets is of great significance for revealing the mechanism of bladder cancer and for the development of more targeted drugs.

In conclusion, Erianin exerts a prominent inhibitory effect on bladder cancer cell growth by inducing G2-M phase arrest and apoptosis. We demonstrated that Erianin-induced apoptosis is primarily associated with the mitochondria-mediated intrinsic apoptosis pathway. Additionally, JNK pathway activation contributes to the anti-proliferation and apoptosis induction effects of Erianin. These findings provide a scientific rationale for the clinical use of Erianin for bladder cancer treatment, and the low toxicity of Erianin indicates that it might be a safe and effective agent for bladder cancer prevention. Of course, Erianin derivatives or newly identified Erianin targets

could also provide new therapeutic strategies for bladder cancer.

Conflicts of interest

The authors have declared no conflicts of interest.

Acknowledgements

The authors sincerely thank all the investigators and coordinators who contributed to this study. This study was financially supported by the National Natural Science Foundation of China (# 81573662, Yaxiong Tang) and the Sichuan Science and Technology Program (No. 2018HH0079).

References

Battenberg, O.A., Yang, Y., Verhelst, S.H., Sieber, S.A., 2013. Target profiling of 4-hydroxyderricin in S. aureus reveals seryl-tRNA synthetase binding and inhibition by covalent modification. Mol Biosyst. 9, 343-351.

Chen, W., Zheng, R., Baade, P.D., Zhang, S., Zeng, H., Bray, F., Jemal, A., Yu, X.Q., He, J., 2016. Cancer statistics in China, 2015. CA Cancer J Clin. 66, 115–132.

Chen, M., Wang, J., 2002. Initiator caspases in apoptosis signaling pathways. Apoptosis. 7, 313-319.

Cushman M., Nagarathnam D., Gopal D., et al. Synthesis and evaluation of stilbene and dihydrostilbene derivatives as potential anticancer agents that inhibit tubulin polymerization. J Med Chem, 1991, 34, 2579-2588.

Charoenrungruang, S., Chanvorachote, P., Sritularak, B., Pongrakhananon, V., 2014. Gigantol, a bibenzyl from Dendrobium draconis, inhibits the migratory behavior of non-small cell lung cancer cells. J Nat Prod. 77(6), 1359-66.

Chen, F., 2012. JNK-induced apoptosis, compensatory growth, and cancer stem cells.

Cancer Res. 72, 379-386.

Davison, E.K., Brimble M.A., 2019. Natural product derived privileged scaffolds in drug discovery. Curr Opin Chem Biol. 52, 1-8.

Elmore, S., 2007. Apoptosis: a review of programmed cell death. Toxicol Pathol. 35, 495-516.

Gu, Q., Wang, J.D., Xia, H.H., Lin, M.C., He, H., Zou, B., Tu, S.P., Yang, Y., Liu, X.G., Lam, S.K., Wong, W.M., Chan, A.O., Yuen, M.F., Kung, H.F., Wong, B.C., 2005. Activation of the caspase-8/Bid and Bax pathways in aspirin-induced apoptosis in gastric cancer. Carcinogenesis. 26, 541-546.

Gupta, S., Afaq, F., Mukhtar, H., 2001. Selective growth-inhibitory, cell-cycle deregulatory and apoptotic response of apigenin in normal versus human prostate carcinoma cells. Biochem Biophys Res Commun. 287, 914–20.

Gong, Y.Q., Fan, Y., Wu, D.Z., Yang, H., Hu, Z.B., Wang, Z.T., 2004. In vivo and in vitro evaluation of erianin, a novel anti-angiogenic agent. Eur J Cancer. 40, 1554-65.

Huang, K. W., Li, Y. R., Tao, S. C., Wei, G., Huang, Y. C., Chen, D. F., et al., 2016. Purification, characterization and biological activity of polysaccharides from Dendrobium officinale. Molecules. 21, 701.

Jin, D., Cao, M., Mu, X., Yang, G., Xue, W., Huang, Y., Chen, H., 2015. Catalpol inhibited the proliferation of T24 human bladder cancer cells by inducing apoptosis through the blockade of Akt-mediated anti-apoptotic signaling. Cell Biochem Biophys. 71, 1349–1356.

Jemal, A., Siegel, R., Ward, E., Hao, Y., Xu, J., Murray, T., Thun, M.J., 2008. Cancer statistics. CA Cancer J Clin. 58, 71-96.

Jones, A., Crew, J., 2000. Vascular endothelial growth factor and its correlation with superficial bladder cancer recurrence rates and stage progression. Urol Clin North Am. 27, 191–197.

Krishnamurthy, A., Jimeno, A., 2017. Atezolizumab: A novel PD-L1 inhibitor in cancer therapy with a focus in bladder and non-small cell lung cancers. Drugs Today (Barc). 53, 217-237.

Kalimuthu, S., Se-Kwon, K., 2013. Cell survival and apoptosis signaling as therapeutic target for cancer: marine bioactive compounds. Int J Mol Sci. 14, 2334-2354.

Kantari, C., Walczak, H., 2011. Caspase-8 and bid: caught in the act between death receptors and mitchondria. Biochim Biophys Acta. 1813, 558-563.

Kaufmann, T., Strasser, A., Jost, P.J., 2012. Fas death receptor signalling: roles of Bid and XIAP. Cell Death Differ. 19, 42-50.

Kim, M.S., Kim, J.E., Lim, D.Y., Huang, Z., Chen, H., Langfald, A., Lubet, R.A., Grubbs, C.J., Dong, Z., Bode, A.M., 2014. Naproxen induces cell cycle arrest and apoptosis in human urinary bladder cancer cell lines and chemically induced cancers by targeting PI3K. Cancer Prev Res (Phila). 7, 236–245.

Li, M,. He, Y,. Peng, C,. Xie, X,. Hu G,. 2018. Erianin inhibits human cervical cancer cell through regulation of tumor protein p53 via the extracellular signal-regulated kinase signaling pathway. Oncol Lett. 16(4):5006-5012.

Li, Y.M., Wang, H.Y., Liu, G.Q., 2001. Erianin induced apoptosis in human leukemia HL-60 cells. Acta pharmacologica Sin. 22, 1018-1022.

Li, M., Zhang, K.Y., But, P.P., Shaw, P.C., 2011. Forensically informative nucleotide sequencing (FINS) for the authentication of Chinese medicinal materials. Chin Med. 6, 42.

Li, C., Fu, S.B., Liu, H.L., Ma, X.R., 2007. Research advances on Apoptosis. World Sci-Thch R&D. 29, 45-53.

Lai, B., Pu, H., Cao, Q., Jing, H., Liu, X., 2011. Activation of Caspase-3 and c-Jun NH2-terminal kinase signaling pathways involving heroin- induced neuronal apoptosis. Neurosci Lett. 502, 209-213.

Marta, G.N., Hanna, S.A., Gadia, R., Correa, S.F., Silva, J.L., Carvalho Hde, A., 2012. The role of radiotherapy in urinary bladder cancer: current status. Int Braz J Urol. 38, 144–153.

Marani, M., Tenev, T., Hancock, D., Downward, J., Lemoine, N.R., 2002. Identification of novel isoforms of the BH3 domain protein Bim which directly activate Bax to trigger apoptosis. Mol Cell Biol. 22, 3577-3589.

Ma, G.X., Xu, G.J., Xu, L.S., Wang, Z.T., Jiu, C.C., 1994. Studies on chemical constituents of *Dendrobium chrysotoxum*. Lindl Acta Pharm Sin. 29, 763-6.

Ma, G.X., Xu, G.J., Xu, L.S., Wang, Y.X., 1994. Inhibitory effects of *Dendrobium chrysotoxum* and its constituents on the mouse HePA and ESC. J China Pharm Univ. 25, 188-9.

Ng, T.B., Liu, J., Wong, J.H., Ye, X., Wing, Sze. S.C., Tong, Y., Zhang, K.Y., 2012. Review of research on Dendrobium, a prized folk medicine. Appl Microbiol Biotechnol. 93, 1795–1803.

Ohtsuka, T., Buchsbaum, D., Oliver, P., Makhija, S., Kimberly, R., Zhou, T., 2003. Synergistic induction of tumor cell apoptosis by death receptor antibody and chemotherapy agent through JNK/p38 and mitochondrial death pathway. Oncogene. 22, 2034-2044.

Parkin, D.M., 2008. The global burden of urinary bladder cancer. Scand J Urol Nephrol Suppl. 218, 12–20.

Prasad, R., Koch, B., 2014. Antitumor activity of ethanolic extract of Dendrobium

formosum in T-cell lymphoma: an in vitro and in vivo study. Biomed Res Int. 2014, 753451.

Rabilloud, T., Lelong, C., 2011. Two-dimensional gel electrophoresis in proteomics: a tutorial. J Proteomics. 74, 1829−1841.

Siegel, R.L., Miller, K.D., Jemal, A., 2017. Cancer statistics. CA Cancer J Clin. 67, 7–30.

Sawada, M., Nakashima, S., Banno, Y., Yamakawa, H., Hayashi, K., Takenaka, K., Nishimura, Y., Sakai, N., Nozawa, Y., 2000. Ordering of ceramide formation, caspase activation, and Bax/Bcl-2 expression during etoposide-induced apoptosis in C6 glioma cells. Cell Death Differ. 7, 761-772.

Son, Y., Cheong, Y.K., Kim, N.H., Chung, H.T., Kang, D.G., Pae, H.O., 2011. Mitogen-Activated Protein Kinases and Reactive Oxygen Species: How Can ROS Activate MAPK Pathways? J Signal Transduct. 2011, 792639.

Shi, Y., 2002. Mechanisms of Caspase Activation and Inhibitong during Apoptosis. Mol Cell. 9, 459-470.

Shaltiel, IA., Krenning, L., Bruinsma, W., Medema, RH. The same, only different - DNA damage checkpoints and their reversal throughout the cell cycle. J Cell Sci. 2015, 128(4):607-20.

Tobiume K, Matsuzawa A, Takahashi T, Nishitoh H, Morita K, Takeda K, Minowa O, Miyazono K, Noda T, Ichijo H. ASK1 is required for sustained activation of JNK/p38 MAP kinases and apoptosis. EMBO Rep. 2001; 2(3): 222-228.

Teixeira da Silva, J.A., Zeng, S., Galdiano, R.F. Jr., Dobránszki, J., Cardoso, J.C., Vendrame, W.A., 2014. In vitro conservation of Dendrobium germplasm. Plant Cell Rep. 33, 1413-23

Tang, Y., Simoneau, A.R., Xie, J., Shahandeh, B., Zi, X., 2008. Effects of the kava chalcone flavokawain A differ in bladder cancer Cells with wild-type versus mutant p53. Cancer Prev Res (Phila). 1, 439-451.

Vandeveer, A.J., Fallon, J.K., Tighe, R., Sabzevari, H., Schlom, J., Greiner, J.W., 2016. Systemic Immunotherapy of Non-Muscle Invasive Mouse Bladder Cancer with Avelumab, an Anti-PD-L1 Immune Checkpoint Inhibitor. Cancer Immunol Res. 4, 452-462.

Wang, H., Zhang, T., Sun, W., Wang, Z., Zuo, D., Zhou, Z., Li, S., Xu, J., Yin, F., Hua, Y., Cai, Z., 2016. Erianin induces G2/M-phase arrest, apoptosis, and autophagy via the ROS/JNK signaling pathway in human osteosarcoma cells in vitro and in vivo. Cell Death Dis. 7, e2247.

Wang, Y.F., Jiang, C.C., Kiejda, K.A., Gillespie, S., Zhang, X.D., Hersey, P., 2007. Apoptosis induction in human melanoma cells by inhibition of MEK is caspase-independent and mediated by the Bcl-2 family members PUMA, Bim,

and Mcl-1. Clin. Cancer Res. 13, 4934–4942.

Wright, M.H., Sieber, S.A., 2016. Chemical proteomics approaches for identifying the cellular targets of natural products. Nat Prod Rep. 33, 681-708.

Yuan, Y., Liu, X., Wang, J., Zhang, J., 2019. Microsc Res Tech. Morphological and microscopic identification of three major medicinal Dendrobium species in Ta-pieh Mountains area. 12.

Yang, P.Y., Liu, K., Ngai, M.H., Lear, M.J., Wenk, M.R., Yao, S.Q., 2010. Activity-based proteome profiling of potential cellular targets of Orlistat--an FDA-approved drug with anti-tumor activities.J Am Chem Soc. 132, 656-666.

Yu, Z., Zhang, T., Gong, C., Sheng, Y., Lu, B., Zhou, L., Ji, L., Wang, Z., 2016. Erianin inhibits high glucose-induced retinal angiogenesis via blocking ERK1/2-regulated HIF-1α-VEGF/VEGFR2 signaling pathway. Sci Rep. 6, 34306.

Zhang, J., Wang, S., Han, F., Li, J., Yu, L., Zhou, P., Chen, Z., Xue, S., Dai, C., Li Q., 2016. MicroRNA-542-3p suppresses cellular proliferation of bladder cancer cells through post-transcriptionally regulating survivin. Gene. 579, 146–152.

Zuo, W., Wang, Z.Z., Xue, J., 2014. Artesunate Induces Apoptosis of Bladder Cancer Cells by miR-16 Regulation of COX-2 Expression. Int J Mol Sci. 15, 14298-14312

Fig. 1: Erianin exerts anti-proliferative effects in human bladder cancer EJ and T24 cells. A. Chemical synthetic schedule of Erianin. B. Cytotoxicity effect of various concentrations of Erianin on EJ, T24, and LO2 cells after 48 h of exposure. MTT assays were performed to examine cell growth (as % viability). Each point is the mean ± SE of three independent experiments. Each bar represents the mean ± SE of three independent experiments. Each sample count was performed in duplicate.

Fig. 2: Effect of Erianin on EJ and T24 cell cycle progression. EJ cells were treated with 0.1% DMSO or 40, 80, or 160 nM Erianin, and T24 cells were treated with 0.1%

DMSO or 25, 50, or 100 nM Erianin. After treatment for 24 h, the cell cycle distribution was analysed by flow cytometry and western blotting. A, B. The cells were stained with propidium iodide for the analysis of cell cycle distribution. Each bar represents the mean ± SE of three independent experiments. C. Western blotting analysis of cell cycle markers in EJ and T24 cells following Erianin treatment. The cell cycle-related proteins p-Chk2, p-cdc2, p-H2A.X and p-cdc25C were analysed using specific antibodies. β-Actin served as the loading control.

Fig. 3: Effect of Erianin on the expression of apoptosis-related proteins. A. The live cell morphology of EJ or T24 cells treated with Erianin at a concentration of 160 nM or 100 nM for 48 h was observed with a phase-contrast light microscope (magnification × 100). DAPI staining was used to visualize the nuclear morphology using a fluorescence microscope (magnification × 200). Control cells were treated with 0.1% DMSO. B. Cells were pretreated in the presence or absence of Z-VAD-FMK (20 μM) for 2 h and treated with Erianin for 24 h. Apoptotic cells were identified through Annexin V-FITC/PI staining. C. The cell cycle distribution after treatment with Z-VAD-FMK (20 μM) and Erianin was analysed by flow cytometry. D. The cells were treated with 0.1% DMSO and Erianin (40, 80, or 160 nM (EJ cells) and 25, 50, or 100 nM (T24 cells)) for 24 h, and the expression of cleaved caspase-9, -7, and -3 and PARP was determined by western blotting. E. The effect of the caspase inhibitor on Erianin-induced apoptosis was measured. Inhibition of caspase activity by Z-VAD-FMK (20 μM) decreased the anti-proliferative effect of Erianin in EJ and

T24 cells. Each bar represents the mean ± SE of three independent experiments. Each point is the mean ± SE of three independent experiments.

Fig. 4: Effect of Erianin on the mitochondrial membrane potential. A. EJ cells were treated with Erianin at a concentration of 160 nM or 100 nM for 24 h, stained with a fluorescent JC-1 probe, and examined under a fluorescence microscope (magnification × 200). B. EJ cells were treated with 0.1% DMSO and various Erianin concentrations (40, 80, or 160 nM). After 24 h of treatment, the mitochondrial membrane potential was analysed by flow cytometry. C. Mitochondrial (m) and cytosolic (c) extracts were prepared, and western blotting was performed as described in the "Materials and Methods" section. β-Actin served as the loading control.

Fig. 5: Effect of Erianin on the expression of Bcl-2 family proteins**.** A. Bim, Bik, Bax, Bad, BID, Mcl-1 and Bcl-2 protein expression after treatment with Erianin at different concentrations (40, 80, and 160 nM (EJ cells) and 25, 50, and 100 nM (T24 cells)) was assessed by western blotting. B. EJ and T24 cells transfected with shBim (459) or shLacZ were treated with 0.1% DMSO or the indicated concentration of Erianin for 24 h. The cell viabilities were measured through MTT assays. The knockdown of Bim expression was verified by western blotting. β-Actin was used as the loading control. C. Bcl-2 overexpression suppressed the growth inhibition effect of Erianin. EJ and T24 cells were transiently transfected with pcDNA3.1 and pcDNA3.1/Bcl-2 for 48 h

and then treated with 0.1% DMSO or the indicated dose of Erianin for 24 h. The cell viabilities were determined through MTT assays. Each point is the mean ± SE of three independent experiments. Each bar represents the mean ± SE of three independent experiments. A western blot analysis of Bcl-2 overexpression in EJ and T24 cells was performed.

Fig. 6: Erianin induced apoptosis by activating the JNK signalling pathway. A. The phosphorylation levels of JNK, Bcl-2 (ser70) and c-Jun proteins in cells after treatment with Erianin and SP600125 (10 μM) for 24 h were analysed by western blotting. β-Actin was used as the loading control. B. The effect of the JNK inhibitor (SP600125) on Erianin-induced apoptosis was measured. Inhibition of JNK activity by SP600125 decreased the anti-proliferation effect of Erianin in EJ and T24 cells. C. The dominant negative mutant c-Jun decreased the proliferation inhibition effect of Erianin in EJ cells. The expression of the dominant negative mutant c-Jun with a His-tag was determined by western blotting. β-Actin was used as the loading control. D. The cell cycle distribution after treatment with SP600125 and Erianin was analysed by flow cytometry. E. The cells were pretreated in the presence or absence of SP600125 for 2 h and treated with Erianin for 24 h, and the apoptotic cells were analysed after annexin V-FITC/PI staining. Each point is the mean ± SE of four independent experiments. Each bar represents the mean ± SE of three independent experiments.

Fig. 7: Erianin reduced EJ cell-derived tumour growth in a xenograft model. A. Mice with bladder tumours were randomly divided into control and treatment groups, with ten mice in each group, and dosed daily with vehicle or Erianin at 50 mg/kg. The tumour volumes were measured, and the results are presented as the means ± SEs. B. At the termination of the study, the tumours were excised from each mouse and weighed. The wet weight of the tumours is presented as the mean of 10 tumours from the individual mice in each group. Bars, ± SEs. C. DNA fragmentation in tumour sections was detected with TUNEL staining. D. Haematoxylin and eosin staining of tumour sections from the vehicle control and Erianin (50 mg/kg) groups was performed, and the results were observed with a fluorescence microscope (magnification × 200).

Highlights

- Erianin exhibited significant anti-proliferative effect in bladder cancer cells.
- Erianin induced G2/M arrest by regulating the expression of cell cycle markers.
- Erianin induced mitochondrial-mediated apoptosis.
- Erianin induced apoptosis via JNK pathway activation.
- Erianin reduced tumour growth in xenograft model and the inhibition ratio was 65%.

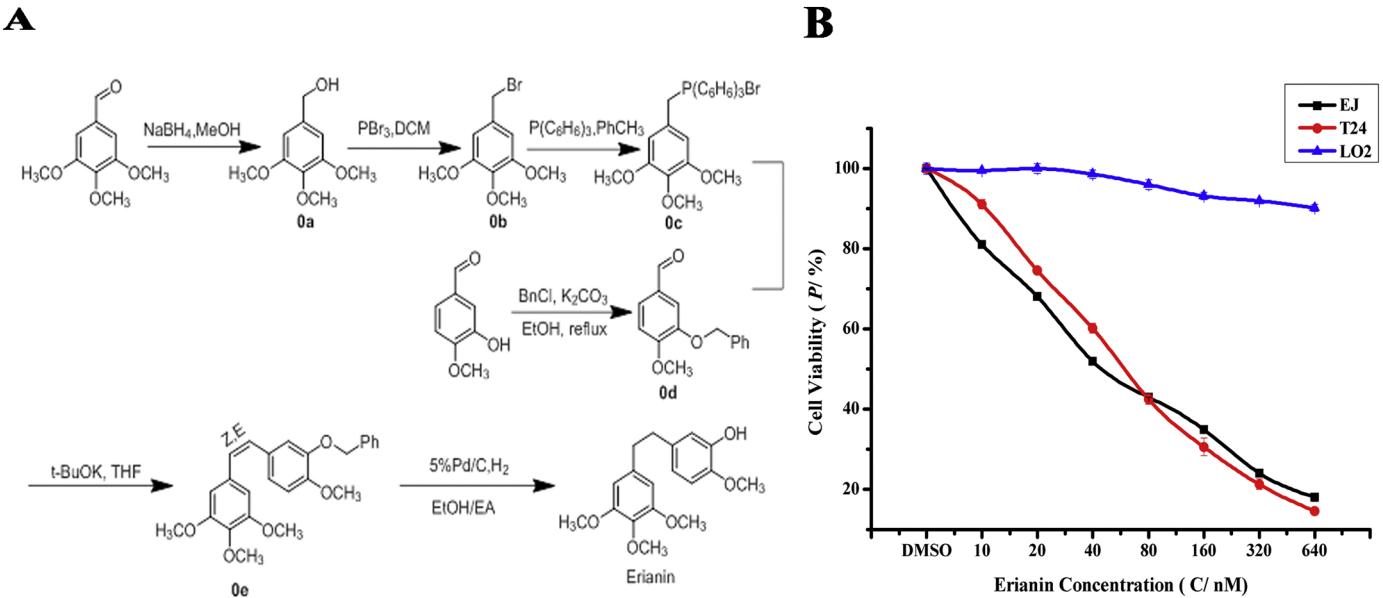
A
NaBH4,MeOH
PBr3,DCM
P(C6H6)3,PhCH3
P(C6H6)3Br
Br
OH
0a
0b
0c
BnCl, K2CO3
EtOH, reflux
Ph
0d
t-BuOK, THF
Z,E
5%Pd/C,H2
EtOH/EA
0e
Erianin
B
EJ
T24
LO2
Cell Viability (P/ %)
100
80
60
40
20
DMSO
10
20
40
80
160
320
640
Erianin Concentration (C/ nM)

Figure 1

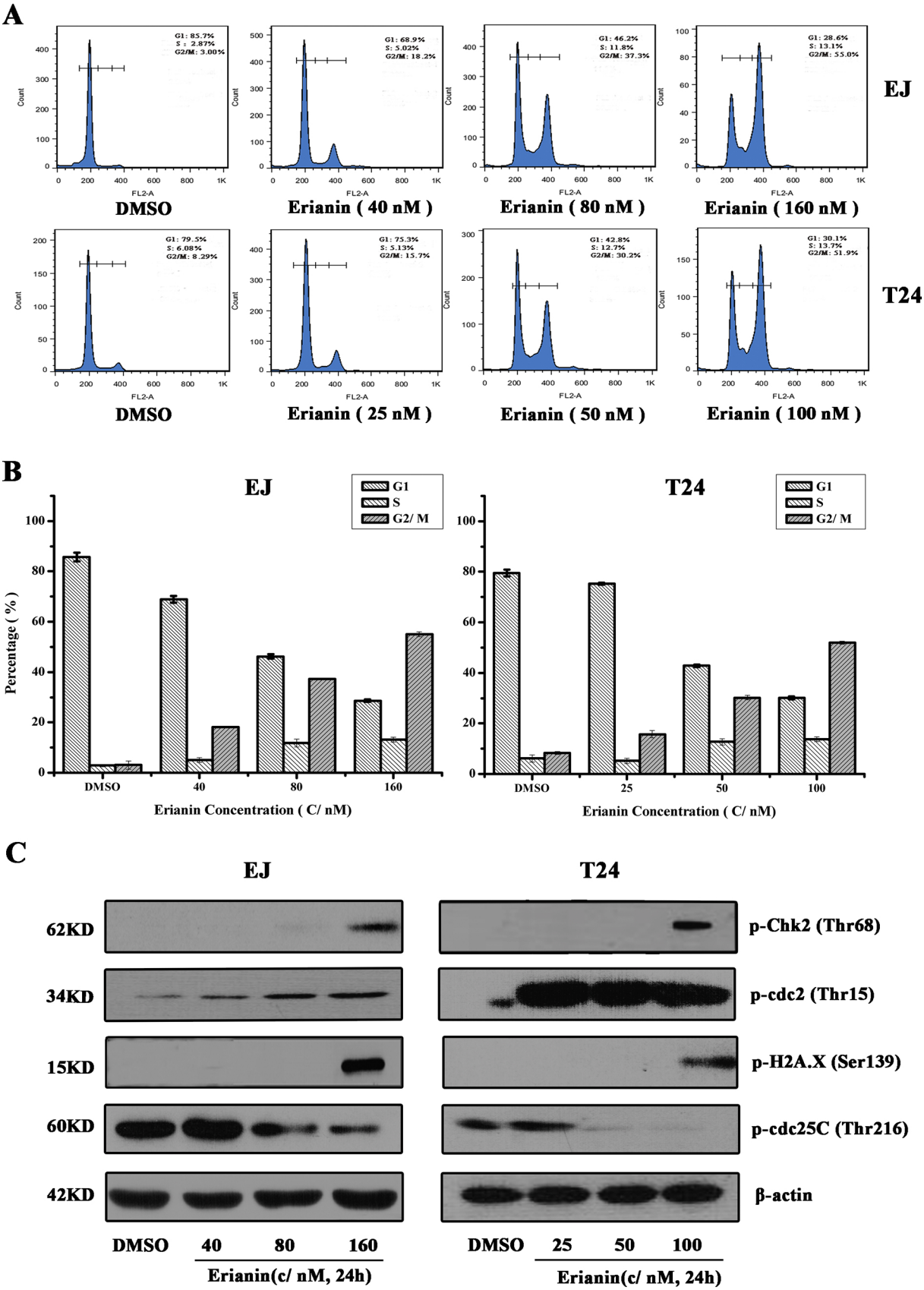
A
EJ
T24
DMSO
Erianin (40 nM)
Erianin (80 nM)
Erianin (160 nM)
Erianin (25 nM)
Erianin (50 nM)
Erianin (100 nM)
G1: 85.7%
S: 2.87%
G2/M: 3.00%
G1: 68.9%
S: 5.02%
G2/M: 18.2%
G1: 46.2%
S: 11.8%
G2/M: 37.3%
G1: 28.6%
S: 13.1%
G2/M: 55.0%
G1: 79.5%
S: 6.08%
G2/M: 8.29%
G1: 75.3%
S: 5.13%
G2/M: 15.7%
G1: 42.8%
S: 12.7%
G2/M: 30.2%
G1: 30.1%
S: 13.7%
G2/M: 51.9%
Count
FL2-A
B
EJ
T24
G1
S
G2/ M
Percentage (%)
Erianin Concentration (C/ nM)
C
62KD
34KD
15KD
60KD
42KD
p-Chk2 (Thr68)
p-cdc2 (Thr15)
p-H2A.X (Ser139)
p-cdc25C (Thr216)
β-actin
Erianin(c/ nM, 24h)

Figure 2

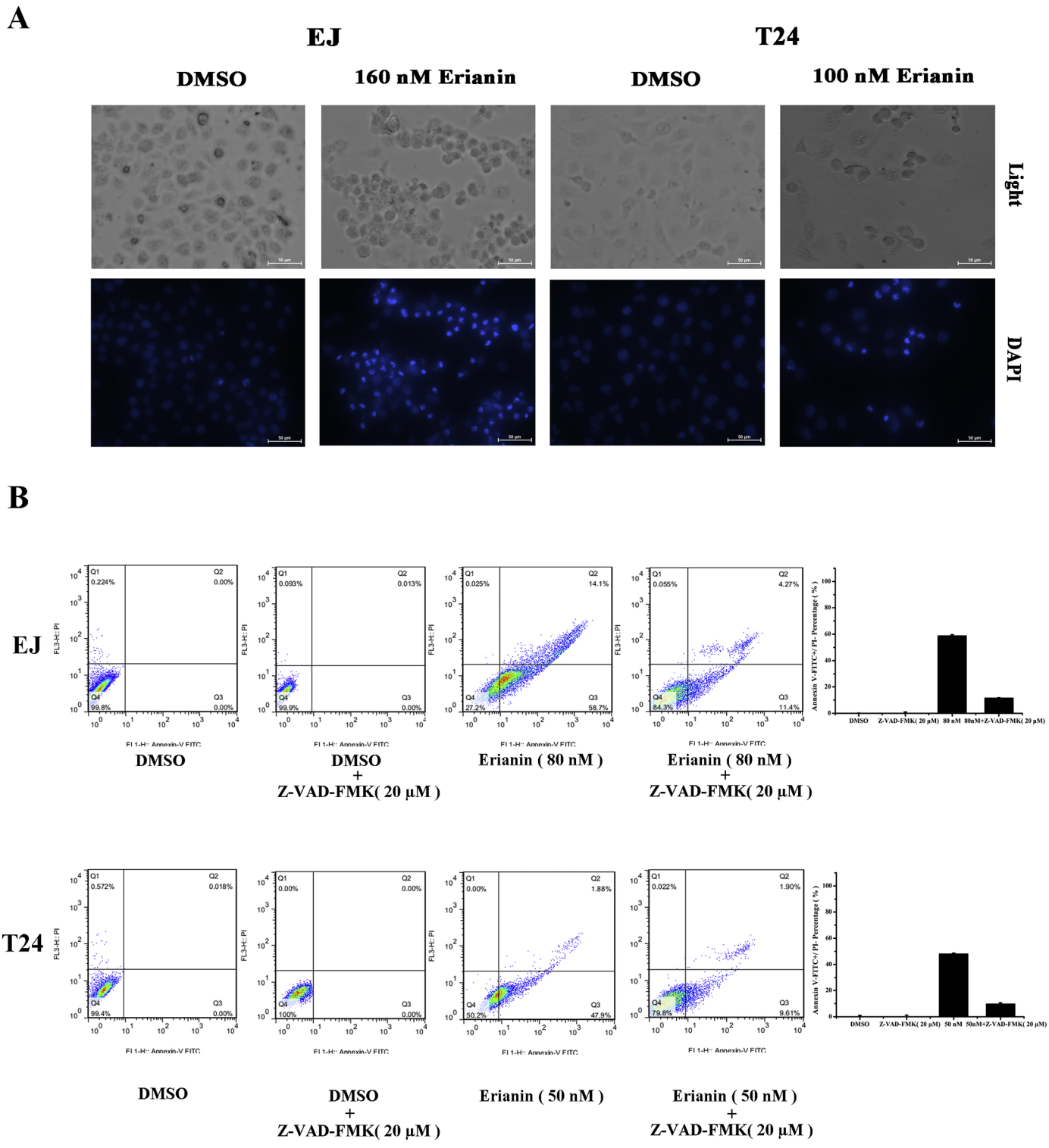
A
EJ
T24
DMSO
160 nM Erianin
DMSO
100 nM Erianin
Light
DAPI
B
EJ
Q1 0.224%
Q2 0.00%
Q4 99.8%
Q3 0.00%
Q1 0.093%
Q2 0.013%
Q4 99.9%
Q3 0.00%
Q1 0.025%
Q2 14.1%
Q4 27.2%
Q3 58.7%
Q1 0.055%
Q2 4.27%
Q4 84.3%
Q3 11.4%
FL3-H:: PI
FL1-H:: Annexin-V FITC
Annexin V-FITC+/ PI- Percentage (%)
DMSO
Z-VAD-FMK(20 μM)
80 nM
80nM+Z-VAD-FMK(20 μM)
DMSO
DMSO + Z-VAD-FMK(20 μM)
Erianin (80 nM)
Erianin (80 nM) + Z-VAD-FMK(20 μM)
T24
Q1 0.572%
Q2 0.018%
Q4 99.4%
Q3 0.00%
Q1 0.00%
Q2 0.00%
Q4 100%
Q3 0.00%
Q1 0.00%
Q2 1.88%
Q4 50.2%
Q3 47.9%
Q1 0.022%
Q2 1.90%
Q4 79.8%
Q3 9.61%
50 nM
50nM+Z-VAD-FMK(20 μM)
DMSO
DMSO + Z-VAD-FMK(20 μM)
Erianin (50 nM)
Erianin (50 nM) + Z-VAD-FMK(20 μM)

Figure 3A

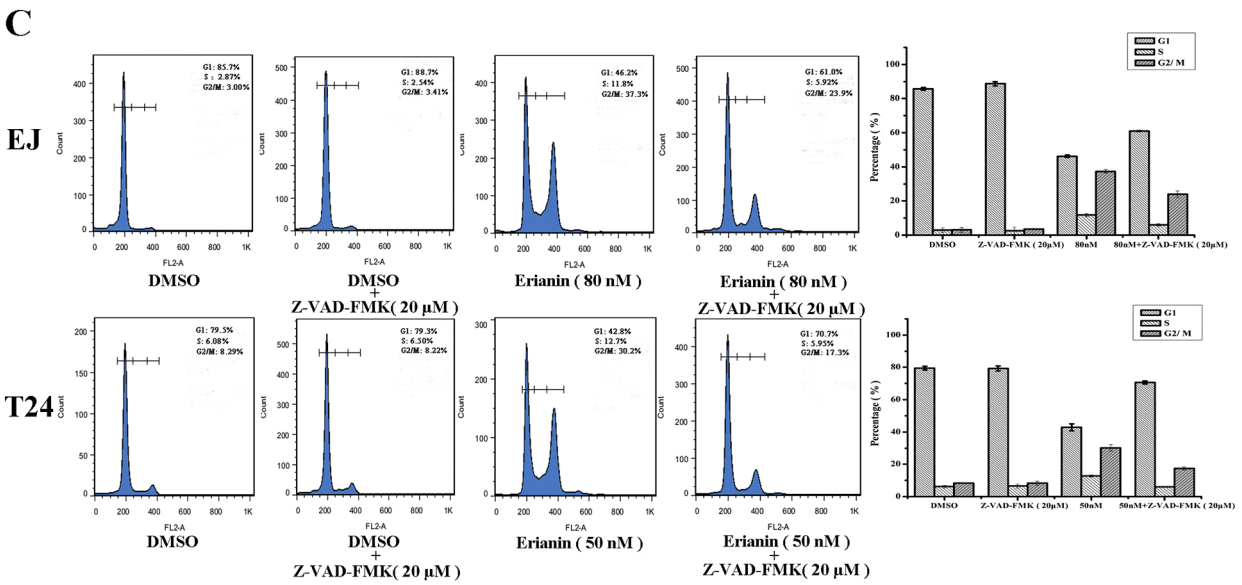
C
EJ
T24
G1: 85.7%
S : 2.87%
G2/M: 3.00%
G1: 88.7%
S: 2.54%
G2/M: 3.41%
G1: 46.2%
S: 11.8%
G2/M: 37.3%
G1: 61.0%
S: 5.92%
G2/M: 23.9%
G1: 79.5%
S: 6.08%
G2/M: 8.29%
G1: 79.3%
S: 6.50%
G2/M: 8.22%
G1: 42.8%
S: 12.7%
G2/M: 30.2%
G1: 70.7%
S: 5.95%
G2/M: 17.3%
Count
FL2-A
Percentage (%)
G1
S
G2/ M
DMSO
DMSO + Z-VAD-FMK(20 μM)
Erianin (80 nM)
Erianin (80 nM) + Z-VAD-FMK(20 μM)
Erianin (50 nM)
Erianin (50 nM) + Z-VAD-FMK(20 μM)
Z-VAD-FMK (20μM)
80nM
80nM+Z-VAD-FMK (20μM)
50nM
50nM+Z-VAD-FMK (20μM)

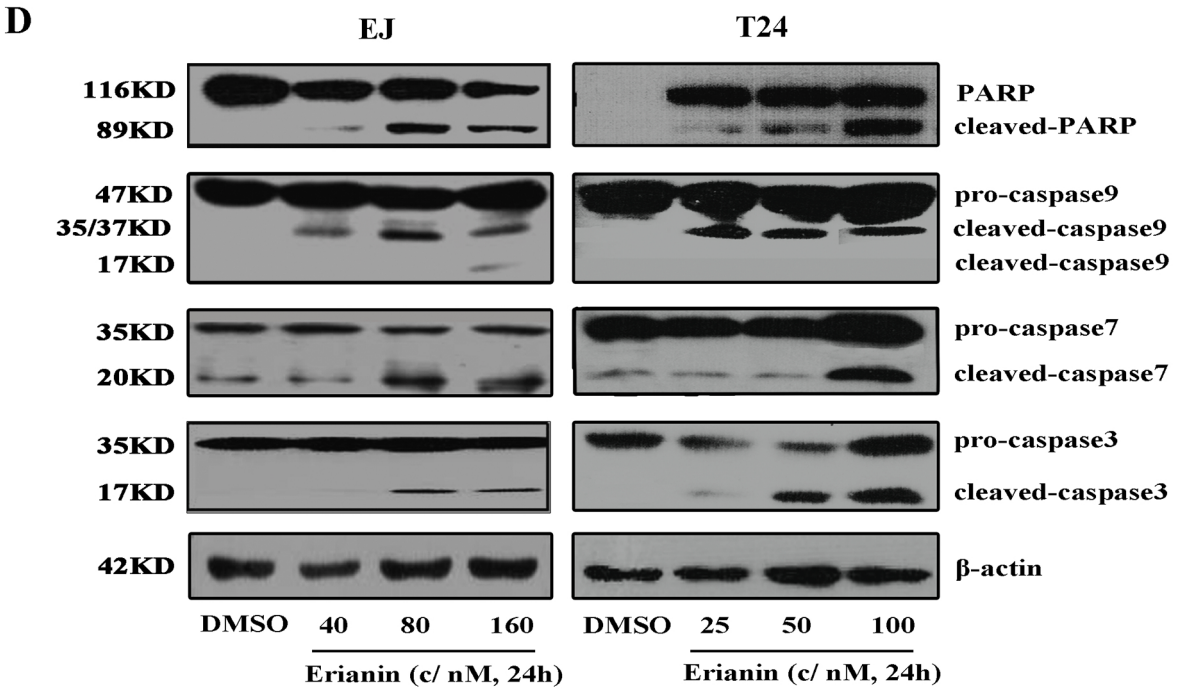
D
EJ
T24
116KD
89KD
PARP
cleaved-PARP
47KD
35/37KD
17KD
pro-caspase9
cleaved-caspase9
cleaved-caspase9
35KD
20KD
pro-caspase7
cleaved-caspase7
35KD
17KD
pro-caspase3
cleaved-caspase3
42KD
β-actin
DMSO 40 80 160
DMSO 25 50 100
Erianin (c/ nM, 24h)
Erianin (c/ nM, 24h)

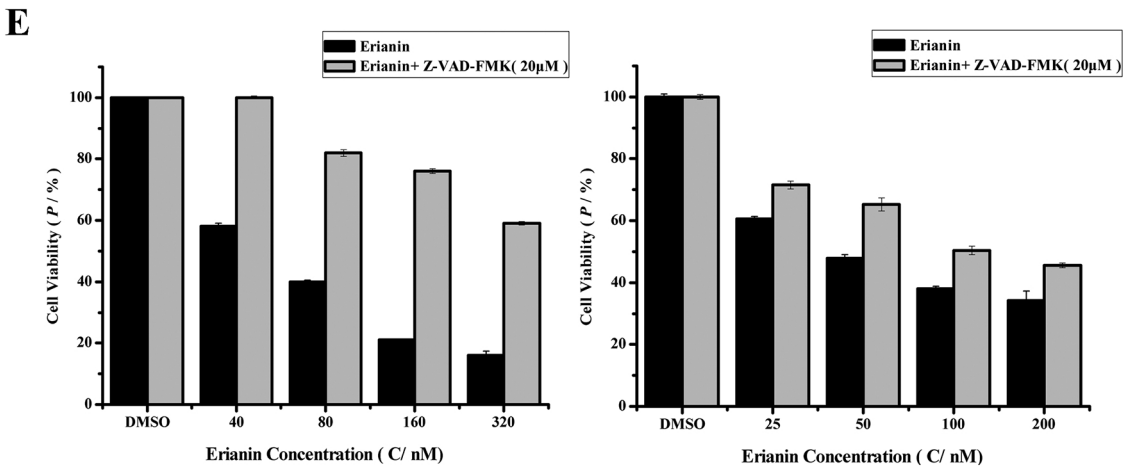
E
Erianin
Erianin+ Z-VAD-FMK(20μM)
Cell Viability (P / %)
DMSO 40 80 160 320
Erianin Concentration (C/ nM)
DMSO 25 50 100 200
Erianin Concentration (C/ nM)

Figure 3B

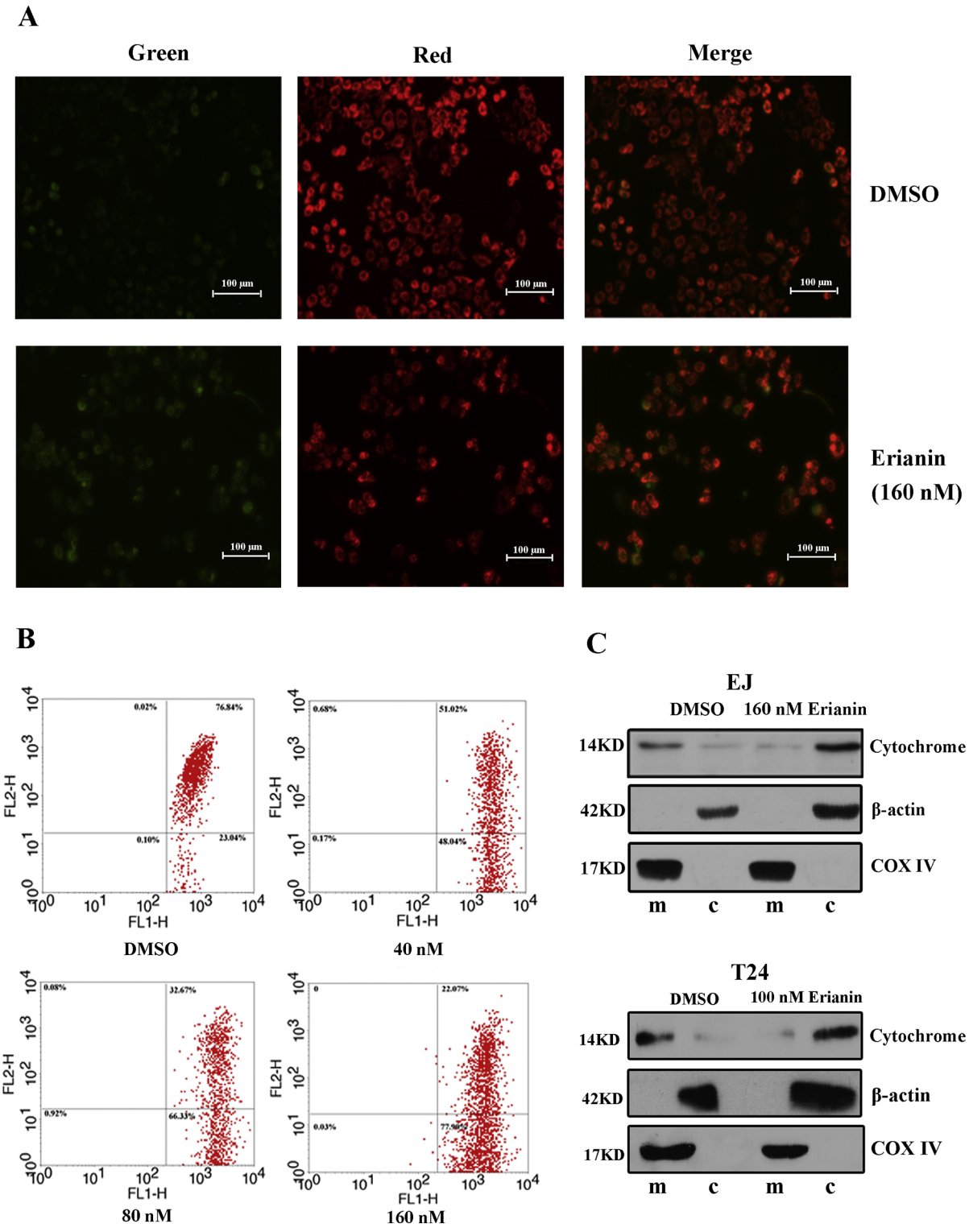
A
Green
Red
Merge
DMSO
Erianin
(160 nM)
100 μm
B
DMSO
40 nM
80 nM
160 nM
FL2-H
FL1-H
0.02%
76.84%
0.10%
23.04%
0.68%
51.02%
0.17%
48.04%
0.08%
32.67%
0.92%
66.33%
0
22.07%
0.03%
C
EJ
DMSO
160 nM Erianin
14KD
42KD
17KD
Cytochrome c
β-actin
COX IV
m
c
T24
100 nM Erianin

Figure 4

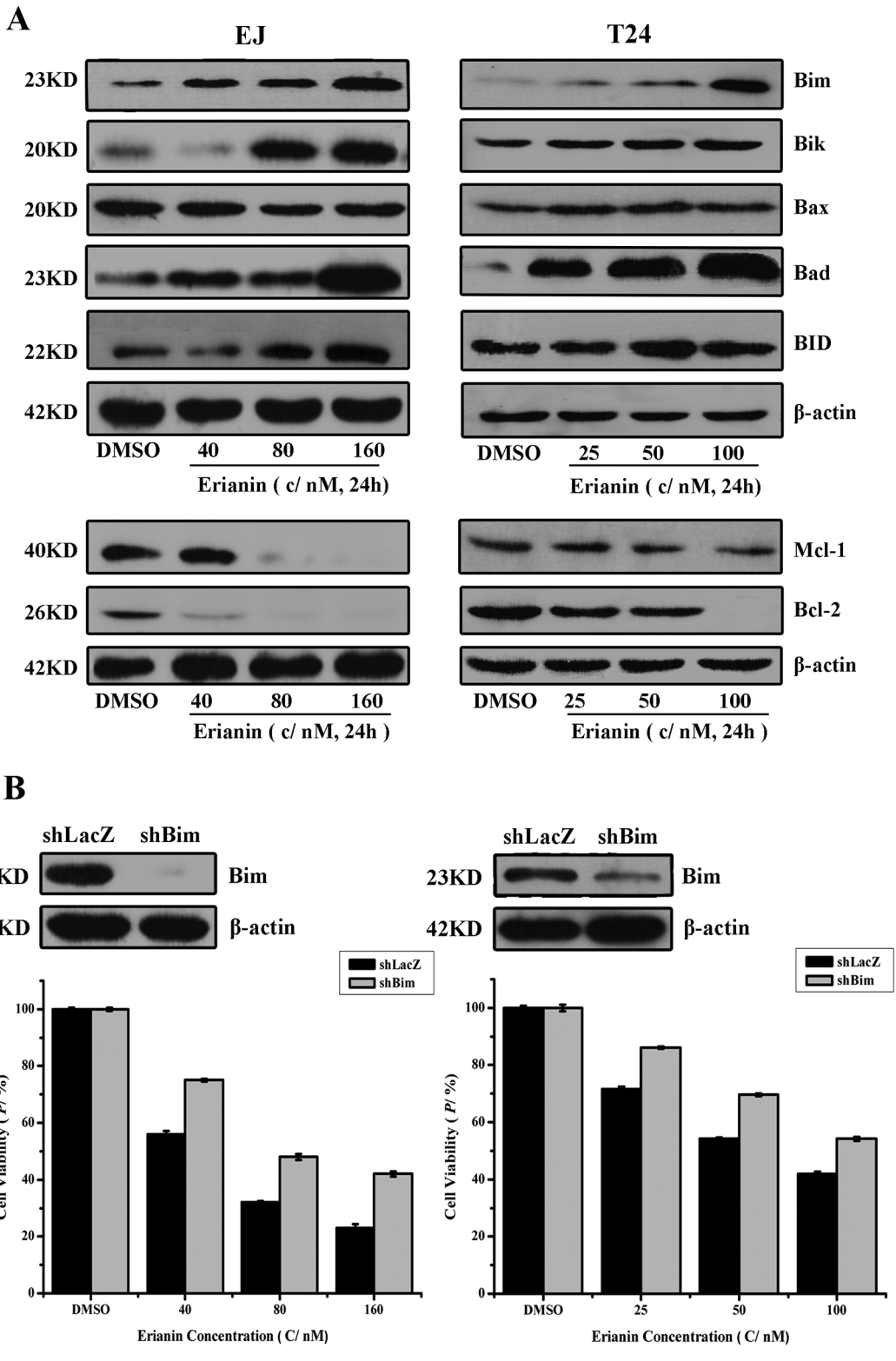
A
EJ
T24
23KD
20KD
20KD
23KD
22KD
42KD
Bim
Bik
Bax
Bad
BID
β-actin
DMSO 40 80 160
Erianin (c/ nM, 24h)
DMSO 25 50 100
Erianin (c/ nM, 24h)
40KD
26KD
42KD
Mcl-1
Bcl-2
β-actin
DMSO 40 80 160
Erianin (c/ nM, 24h)
DMSO 25 50 100
Erianin (c/ nM, 24h)
B
shLacZ shBim
23KD
42KD
Bim
β-actin
shLacZ
shBim
Cell Viability (P/ %)
0 20 40 60 80 100
DMSO 40 80 160
Erianin Concentration (C/ nM)
DMSO 25 50 100
Erianin Concentration (C/ nM)

Figure 5A

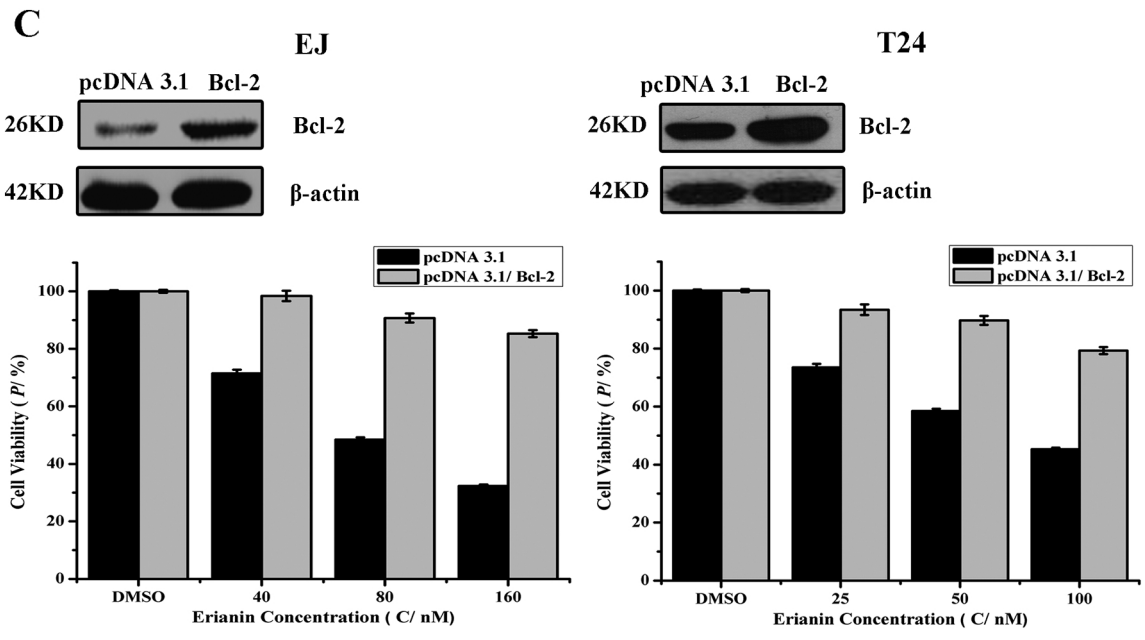
C
EJ
pcDNA 3.1
Bcl-2
26KD
Bcl-2
42KD
β-actin
T24
pcDNA 3.1
Bcl-2
26KD
Bcl-2
42KD
β-actin
pcDNA 3.1
pcDNA 3.1/ Bcl-2
Cell Viability (P/ %)
0
20
40
60
80
100
DMSO
40
80
160
Erianin Concentration (C/ nM)
pcDNA 3.1
pcDNA 3.1/ Bcl-2
Cell Viability (P/ %)
0
20
40
60
80
100
DMSO
25
50
100
Erianin Concentration (C/ nM)

Figure 5B

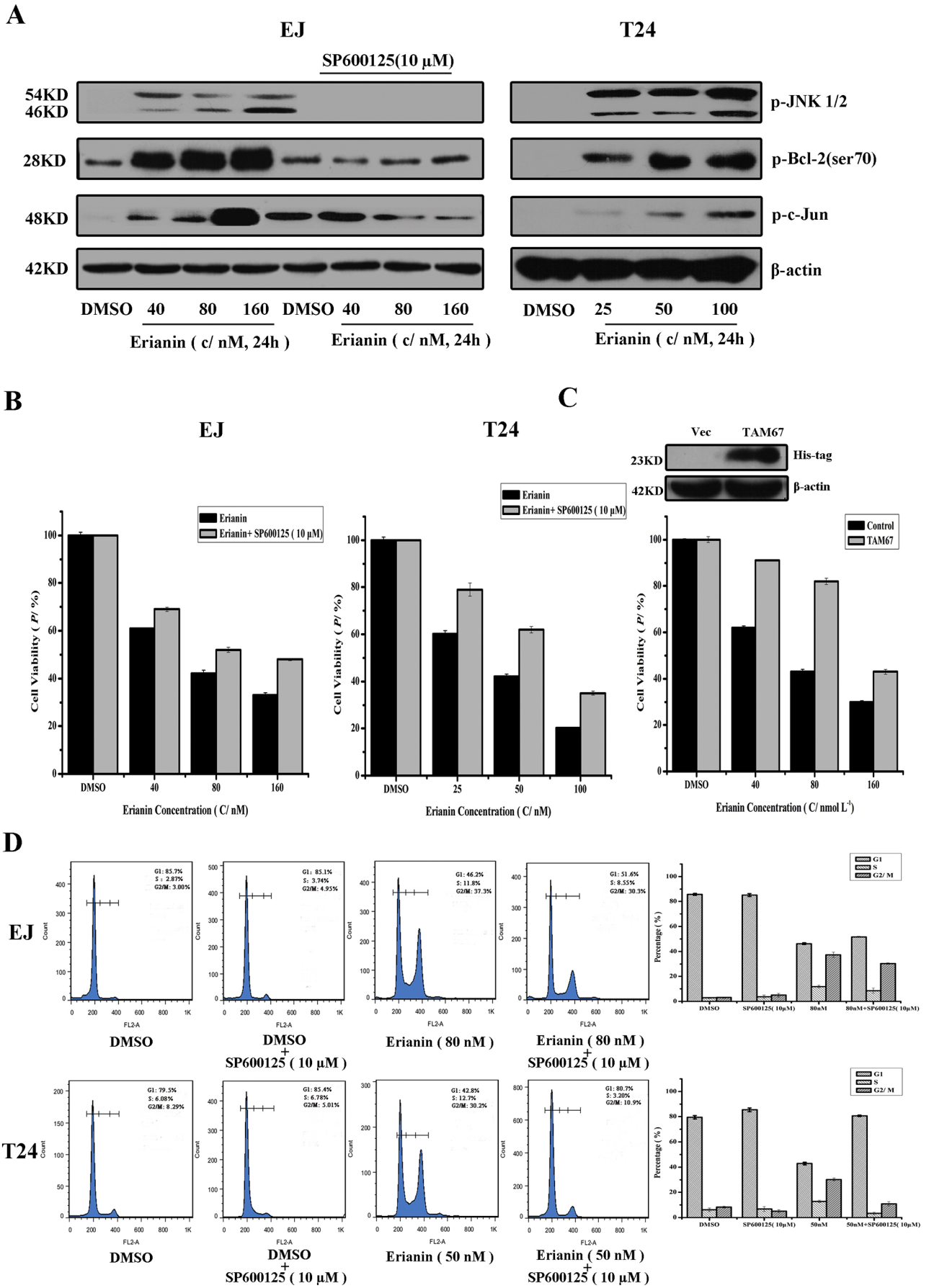
A
EJ
T24
SP600125(10 μM)
54KD
46KD
28KD
48KD
42KD
p-JNK 1/2
p-Bcl-2(ser70)
p-c-Jun
β-actin
DMSO 40 80 160 DMSO 40 80 160
DMSO 25 50 100
Erianin (c/ nM, 24h)
Erianin (c/ nM, 24h)
Erianin (c/ nM, 24h)
B
EJ
T24
Erianin
Erianin+ SP600125 (10 μM)
Cell Viability (P/ %)
Erianin Concentration (C/ nM)
C
Vec
TAM67
23KD
His-tag
42KD
β-actin
Control
TAM67
Cell Viability (P/ %)
Erianin Concentration (C/ nmol L-1)
D
EJ
T24
G1: 85.7%
S : 2.87%
G2/M: 3.00%
G1: 85.1%
S: 3.74%
G2/M: 4.95%
G1: 46.2%
S: 11.8%
G2/M: 37.3%
G1: 51.6%
S: 8.55%
G2/M: 30.3%
G1: 79.5%
S: 6.08%
G2/M: 8.29%
G1: 85.4%
S: 6.78%
G2/M: 5.01%
G1: 42.8%
S: 12.7%
G2/M: 30.2%
G1: 80.7%
S: 3.20%
G2/M: 10.9%
Count
FL2-A
Percentage (%)
G1
S
G2/ M
DMSO
SP600125(10μM)
80nM
80nM+SP600125(10μM)
50nM
50nM+SP600125(10μM)
DMSO
DMSO + SP600125 (10 μM)
Erianin (80 nM)
Erianin (80 nM) + SP600125 (10 μM)
Erianin (50 nM)
Erianin (50 nM) + SP600125 (10 μM)

Figure 6A

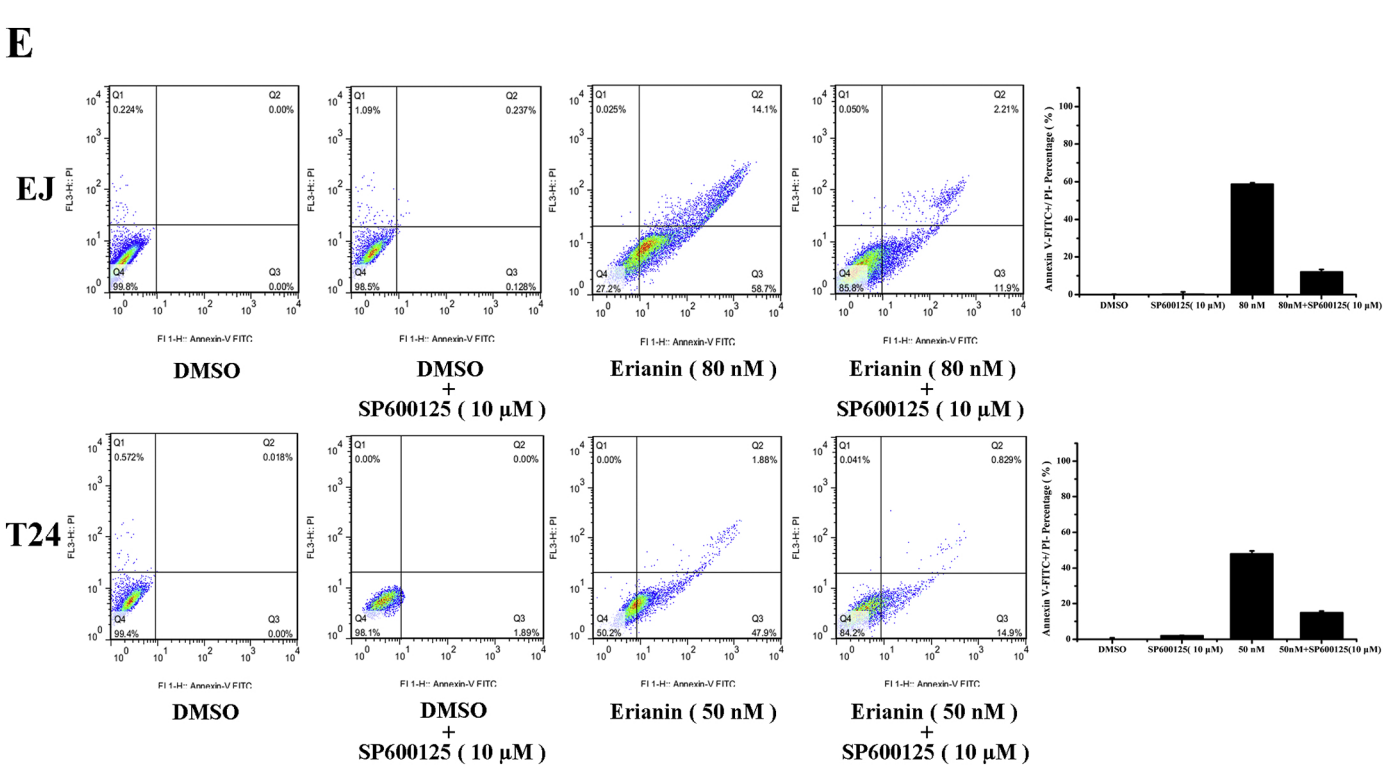
E
EJ
T24
Q1 0.224%
Q2 0.00%
Q4 99.8%
Q3 0.00%
Q1 1.09%
Q2 0.237%
Q4 98.5%
Q3 0.128%
Q1 0.025%
Q2 14.1%
Q4 27.2%
Q3 58.7%
Q1 0.050%
Q2 2.21%
Q4 85.8%
Q3 11.9%
FL3-H:: PI
FL1-H:: Annexin-V FITC
Annexin V-FITC+/ PI- Percentage (%)
DMSO
SP600125(10 μM)
80 nM
80nM+SP600125(10 μM)
DMSO
DMSO + SP600125 (10 μM)
Erianin (80 nM)
Erianin (80 nM) + SP600125 (10 μM)
Q1 0.572%
Q2 0.018%
Q4 99.4%
Q3 0.00%
Q1 0.00%
Q2 0.00%
Q4 98.1%
Q3 1.89%
Q1 0.00%
Q2 1.88%
Q4 50.2%
Q3 47.9%
Q1 0.041%
Q2 0.829%
Q4 84.2%
Q3 14.9%
50 nM
50nM+SP600125(10 μM)
DMSO
DMSO + SP600125 (10 μM)
Erianin (50 nM)
Erianin (50 nM) + SP600125 (10 μM)

Figure 6B

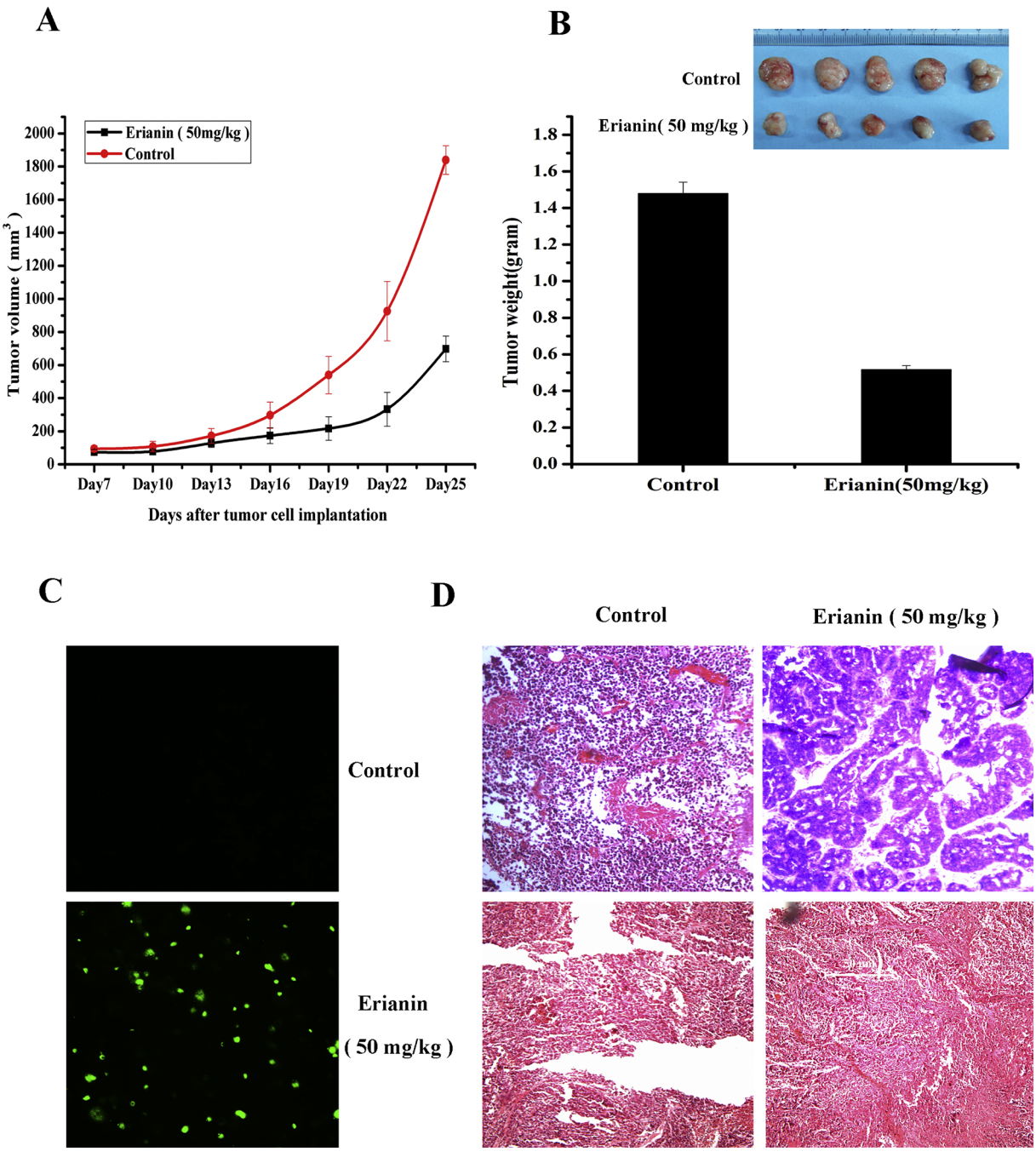
A
Erianin (50mg/kg)
Control
Tumor volume (mm3)
2000
1800
1600
1400
1200
1000
800
600
400
200
0
Day7
Day10
Day13
Day16
Day19
Day22
Day25
Days after tumor cell implantation
B
Control
Erianin(50 mg/kg)
Tumor weight(gram)
1.8
1.6
1.4
1.2
1.0
0.8
0.6
0.4
0.2
0.0
Control
Erianin(50mg/kg)
C
Control
Erianin
(50 mg/kg)
D
Control
Erianin (50 mg/kg)

Figure 7